Check for updates

Earth's Future

RESEARCH ARTICLE
10.1029/2026EF008532

Nitrogen Memoryscapes: Typologies of Nitrogen Inputs and Riverine Loads Across the Continental United States

D. K. Byrnes[1], K. J. Van Meter[2,3], and N. B. Basu[1,4,5]

[1]Department of Civil and Environmental Engineering, University of Waterloo, Waterloo, ON, Canada, [2]Geography Department, The Pennsylvania State University, State College, PA, USA, [3]Earth and Environmental Systems Institute, The Pennsylvania State University, University Park, PA, USA, [4]Department of Earth and Environmental Sciences, University of Waterloo, Waterloo, ON, Canada, [5]The Water Institute, University of Waterloo, Waterloo, ON, Canada

Key Points:

- We analyze long-term relationships between nitrogen surplus and riverine nitrogen load across 490 US watersheds
- Surplus trends do not reliably translate into proportionate changes in nitrogen load, in some cases revealing decoupling of inputs and loads
- Distinct watershed response regimes emerge from interaction among nitrogen management, climate, and legacy nitrogen storage

Supporting Information:

Supporting Information may be found in the online version of this article.

Correspondence to:

D. K. Byrnes and N. B. Basu,
danyka.byrnes@uwaterloo.ca
nandita.basu@uwaterloo.ca

Citation:

Byrnes, D. K., Van Meter, K. J., & Basu, N. B. (2026). Nitrogen memoryscapes: Typologies of nitrogen inputs and riverine loads across the continental United States. *Earth's Future*, *14*, e2026EF008532. https://doi.org/10.1029/2026EF008532

Received 11 MAR 2026
Accepted 19 JUN 2026

Author Contributions:

Conceptualization: D. K. Byrnes, K. J. Van Meter, N. B. Basu
Data curation: D. K. Byrnes
Formal analysis: D. K. Byrnes
Funding acquisition: D. K. Byrnes, K. J. Van Meter, N. B. Basu
Investigation: D. K. Byrnes, N. B. Basu
Methodology: D. K. Byrnes, K. J. Van Meter, N. B. Basu
Supervision: K. J. Van Meter, N. B. Basu
Visualization: D. K. Byrnes
Writing – original draft: D. K. Byrnes
Writing – review & editing: D. K. Byrnes, K. J. Van Meter, N. B. Basu

© 2026 The Author(s). Earth's Future published by Wiley Periodicals LLC on behalf of American Geophysical Union. This is an open access article under the terms of the Creative Commons Attribution License, which permits use, distribution and reproduction in any medium, provided the original work is properly cited.

Abstract Nitrogen pollution has severely impacted inland and coastal waters, contributing to eutrophication, harmful algal blooms, and drinking water contamination. Reducing nitrogen inputs is widely expected to improve water quality, but watershed responses to changing nitrogen surplus are often nonlinear and delayed, complicating expectations of recovery. Here, we analyze long-term trends in nitrogen surplus and riverine nitrogen loads across 490 US watersheds from 1990 to 2017 to examine how changes in inputs translate into changes in load. By jointly classifying watersheds based on the direction of surplus and load trends, we identify four response regimes that capture the diversity of nitrogen dynamics across US landscapes. Using a multivariate classification framework, we show that watershed responses are shaped by interactions among nitrogen source type, hydrologic connectivity, climate constraints, and legacy nitrogen storage. Livestock density is associated with increasing nitrogen surplus, while declining atmospheric deposition is associated with decreasing surplus and loads. Groundwater-dominated watersheds exhibit increasing nitrogen loads despite declining surplus, reflecting the long memory of subsurface nitrogen storage. Connectivity modulates these responses: tile-drained watersheds exhibit tight coupling between surplus and load, whereas arid, low-connectivity systems show declining loads despite increasing surplus. These results show that spatial patterns in riverine loads cannot be used to infer recovery trajectories following reductions in nitrogen inputs, and effective nitrogen management requires accounting for watershed-specific response regimes.

Plain Language Summary Reducing nitrogen inputs is often expected to improve water quality, but in reality, rivers' load responses vary across watersheds. Using 30 years of data from 490 US watersheds, we show that nitrogen carried by rivers reflects not only current and past nitrogen inputs but also depends on how nitrogen enters the landscape and how nitrogen and water move through it. High livestock density promotes increasing accumulation, tile drainage increases rapid export, and groundwater-dominated systems can continue releasing stored nitrogen long after inputs decline. In contrast, declining atmospheric nitrogen deposition is more directly linked to improving water quality in low-agriculture watersheds. These results highlight the need for watershed-specific nitrogen management strategies.

1. Introduction

Over the last 100 years, population growth has fundamentally altered the global nitrogen cycle through the large-scale introduction of reactive nitrogen into terrestrial and aquatic systems. This transformation has been driven primarily by the expansion of industrial fertilizer production, increased fossil fuel combustion, and widespread land use change (Byrnes et al., 2020; Galloway & Cowling, 2021; Glibert, 2020). Together, these activities have dramatically increased nitrogen inputs to landscapes, often exceeding the capacity of crops, soils, and ecosystems to assimilate or retain applied nitrogen. As a result, substantial nitrogen surpluses have accumulated across many regions, with excess nitrogen stored in soils and groundwater or exported to downstream aquatic systems (Ascott et al., 2017; Basu et al., 2022; Chang et al., 2021; J. Han et al., 2024; Van Meter et al., 2018; Vero et al., 2017).

Excess nitrogen has contributed to various environmental issues, including eutrophication, algal blooms, and contamination of drinking water sources (Díaz & Rosenberg, 2011; Glibert, 2020; Van Meter et al., 2018). In the US alone, excess nitrogen has caused water quality deterioration in over 840,000 km of rivers and streams (U.S. Environmental Protection Agency (USEPA), 2020), and has contributed to large hypoxic zones in offshore coastal regions such as the Gulf of Mexico (Harding et al., 2019; Malone & Newton, 2020; Rabalais et al., 2002). Moreover, it is estimated that approximately 1.4 million people depend on groundwater sources in regions with

23284277, 2026, 8, Downloaded from https://agupubs.onlinelibrary.wiley.com/doi/10.1029/2026EF008532, Wiley Online Library on [03/11/2026]. See the Terms and Conditions (https://onlinelibrary.wiley.com/terms-and-conditions) on Wiley Online Library for rules of use; OA articles are governed by the applicable Creative Commons License

nitrogen concentrations that exceed the safe limits for drinking water (Ransom et al., 2021; Ward et al., 2018). Addressing nitrogen pollution in surface and groundwater systems in the face of a growing population and agricultural intensification is crucial to preserving both water and food security.

To manage nitrogen pollution in surface and groundwater systems, it is important to understand the main climate and landscape drivers of these increased concentrations and loads. This question has been studied for the last two decades, beginning with R. W. Howarth et al. (1996), who found a close linear relationship between the net nitrogen inputs to the landscape and stream nitrogen loads. The slope of this relationship varies across watersheds, from 6% to 40% across the US and Canada (Boyer et al., 2002; Goyette et al., 2016; H. Han & Allan, 2008; Sobota et al., 2009; Swaney et al., 2012), 15% in watersheds draining to the Baltic Sea (Hong et al., 2017), 28% in western Europe (Ehrhardt et al., 2021), and 25%–38% in China (Huishu et al., 2018; Wang et al., 2016). In more recent work, machine learning models developed to predict stream nitrogen export have also shown that spatial patterns of nitrogen export across over 2000 streams in the US are primarily influenced by nitrogen inputs, while precipitation and soil type act as secondary controls (Sadayappan et al., 2022).

Recognition that agricultural nitrogen inputs are a major driver of water-quality degradation has motivated policy and management efforts worldwide to reduce fertilizer use and increase crop yield, thus decreasing net nitrogen inputs and improving nitrogen use efficiency (Basu et al., 2022; R. Howarth et al., 2012; X. Zhang et al., 2021). For example, from 1990 to 2018, net nitrogen inputs across the European Union decreased by 11.8 kg-N ha^{-1} yr^{-1} (29%) following the implementation of the Nitrate Directive (Batool et al., 2022; Bouraoui & Grizzetti, 2011). Similarly, parts of the eastern United States have experienced decreases in net nitrogen inputs ranging from 2.5 to 50 kg-N ha^{-1} yr^{-1} over 10 years (Byrnes et al., 2020; Sabo et al., 2019). In China, the net nitrogen inputs in the north central region of the Yellow Basin have plateaued at 80 kg-N ha^{-1} yr^{-1} after a 2004 peak (Pei et al., 2022), while other areas have increasing net inputs (Y. Han et al., 2020).

In some watersheds, reductions in nitrogen inputs have translated into measurable improvements in water quality, consistent with relatively direct input-output relationships (Basu et al., 2022). For example, we see this in the Odense River basin in Denmark and Appomattox River in the Chesapeake River basin (Basu et al., 2022; Chang et al., 2021). However, in many systems, changes in nitrogen inputs have not resulted in proportional or timely decreases in riverine nitrogen load. For instance, in China's Songhuajiang River Basin and Raohe River Basin, nitrogen inputs decreased by 3 and 7 kg-N ha^{-1} yr^{-1}, respectively, over the last decade, yet nitrogen loads continued to increase in both watersheds, with the Raohe River Basin having an increase of 17 kg-N ha^{-1} yr^{-1} (Gao et al., 2023; Zhong et al., 2022). In the Susquehanna watershed in the US, inputs plateaued around 40 kg-N ha^{-1} yr^{-1} from the 1970s to mid-2000s. Despite the plateau of inputs, loads continued to increase during this period from 5 to nearly 8 kg-N ha^{-1} yr^{-1} (Van Meter et al., 2017).

This nonlinear response reflects a hysteresis effect, whereby watershed nitrogen export depends not only on current inputs but also on the legacy of past nitrogen accumulation within soils and groundwater (Basu et al., 2022; Chang et al., 2021; Dupas et al., 2018; Van Meter & Basu, 2017; Van Meter et al., 2023). Across the US, Van Meter et al. (2023) found that approximately one-third of watersheds exhibit clear hysteresis, with nitrogen loads lagging behind changes in inputs. These findings highlight a key distinction between spatial relationships linking nitrogen inputs and loads, and temporal responses to changing inputs: while nitrogen inputs may explain broad spatial patterns in export, reductions in inputs do not necessarily produce immediate declines in nitrogen loads.

Instead, this lagged or hysteretic response is often attributed to legacy nutrients that have accumulated over decades of excess fertilizer application and continue to influence watershed behavior long after inputs change (Basu et al., 2022; Van Meter et al., 2023). Legacy nutrients can accumulate in soils as soil organic nitrogen, also referred to as biogeochemical legacy, or dissolved in pore water and groundwater as hydrologic legacy (Van Meter & Basu, 2015). The challenge is that both the magnitude of these legacy stores and their release rates into the stream are largely unknown, complicating predictions of watershed responses to changing input patterns.

Researchers have attempted to quantify the timescales of watershed response using the metric lag time—the interval between changes in management leading to decreases in the net nitrogen inputs and a measurable decrease in stream export. Such time lags have been quantified across watersheds globally. For example, in a study of 238 watersheds across Western Europe, lag times were found to vary from 0.2 to 34 years, with shorter lag times associated with wetter catchments (Ehrhardt et al., 2021). A study of 16 Canadian catchments found lag

23284277, 2026, 8, Downloaded from https://agupubs.onlinelibrary.wiley.com/doi/10.1029/2026EF008532, Wiley Online Library on [03/11/2026]. See the Terms and Conditions (https://onlinelibrary.wiley.com/terms-and-conditions) on Wiley Online Library for rules of use; OA articles are governed by the applicable Creative Commons License

times varying from 12 to 34 years, influenced by nutrient source and distribution, watershed topography, soil type, climate, and tile-drainage densities, and groundwater travel time (Van Meter & Basu, 2017). We also see lag times spanning approximately 10 years in seven catchments in France (Dupas et al., 2018), ranging from 7 to 22 years in three nested catchments in Germany (Ehrhardt et al., 2019), and from 1 to 12 years in 77 catchments in New Zealand (McDowell et al., 2021). Across these studies, shorter lag times are associated with catchment size, geomorphology, land management changes including tile drainage, and shallower groundwater, while longer lag times are associated with deeper groundwater and low permeability lithology, though substantial variability remains unexplained.

Most existing empirical and modeling studies focus on answering the following question: when nitrogen inputs decrease, how long does it take for riverine nitrogen loads to respond? Implicit in this framing is the assumption that nitrogen inputs are already declining, and the primary uncertainty lies in the lag time before water quality improves. While this perspective has yielded important insights into legacy nitrogen dynamics, it excludes a substantial portion of observed input-load trajectories and leaves several critical scenarios unexplored. These include watersheds where nitrogen inputs are increasing, as well as systems where inputs are decreasing but riverine nitrogen loads continue to rise.

To improve predictions of watershed responses to changing nitrogen inputs and to better inform water-quality management, there is a need for a more comprehensive framework that captures the diversity of nitrogen input-load relationships and identifies the landscape characteristics associated with different response types. Here, we develop a classification framework based on joint trends in nitrogen surplus and riverine nitrogen loads for 490 watersheds across the United States and address the following questions: (a) How have nitrogen inputs and riverine nitrogen loads changed over the past three decades across US watersheds? (b) What relationships emerge between changes in inputs and changes in riverine nitrogen loads? (c) How are climate, land use, and land management characteristics associated with different nitrogen response typologies?

2. Methods

2.1. Data Sources and Site Selection for Streamflow and Nitrogen Concentrations

We analyzed streamflow and nitrate concentration data between 1990 and 2017 across the contiguous US. Streamflow data was obtained from the US Geological Survey's (USGS) National Water Information System (NWIS). Nitrate concentration data were compiled from two different sources to provide continuous temporal coverage: (a) 1965–2012: Oelsner et al. (2017), and (b) 2013–2017: NWIS and Water Quality Portal. The Oelsner et al. (2017) data set was compiled as a part of the United States Geological Survey's National Water-Quality Assessment Project, which paired data from stream gauges and water quality monitoring stations based on proximity along the same stream network. However, the data set ended in 2012, which required us to acquire more recent data for our analysis. We used the watershed IDs compiled by Oelsner et al. (2017) to retrieve data from federal, state, tribal, regional, and local government agencies, and nongovernmental organizations through the dataRetrieval and EGRET packages in R (DeCicco et al., 2021; Hirsch et al., 2021). We then used a set of criteria based on Oelsner et al. (2017) to exclude watersheds with incomplete data: (a) at least 70% of the years had quarterly samples; (b) at least 10% of the samples were taken during high flows; (c) gaps between sampling days were less than 4 years; (d) no more than six consecutive days with missing streamflow per year; (e) no more than 30 days with zero streamflow per year; (f) at least 10 complete years of data were available; and (g) first record began in 2003 or earlier. Some stations that had data discontinuities were included if there was at least a 10-year period that met the above criteria by removing the years before or after the data gaps. These criteria led to a selection of 512 stations used for further analysis.

2.2. Estimation of Daily and Annual Riverine Nitrogen Loads

Daily watershed loads were estimated for each watershed using the Weighted Regressions on Time, Discharge, and Season (WRTDS) approach, which predicts daily concentrations and loads as a function of time, streamflow, and season (Hirsch & DeCicco, 2015; Oelsner et al., 2017). Prior to running WRTDS, the concentration and flow data were cleaned. Specifically, when multiple records were available for a given day, we averaged the multiple records to get a single concentration. We also removed outlier concentrations that were six standard deviations from mean in log space. For stations with discontinuous flow data of 6 days or less, we used linear interpolation between the nearest days to estimate missing flow data. Model performance was evaluated using the flux bias

23284277, 2026, 8, Downloaded from https://agupubs.onlinelibrary.wiley.com/doi/10.1029/2026EF008532, Wiley Online Library on [03/11/2026]. See the Terms and Conditions (https://onlinelibrary.wiley.com/terms-and-conditions) on Wiley Online Library for rules of use; OA articles are governed by the applicable Creative Commons License

metric, and watersheds with a flux bias exceeding ±30% were excluded (Figure S1 in Supporting Information S1). This resulted in the final data set of 490 watersheds. Annual loads were calculated by summing daily loads.

Annual nitrogen loads were used to estimate temporal trends, as described in Section 2.4. Our approach to trend estimation is based on actual nitrogen loads and differs from the flow-normalized trend framework reported by Oelsner et al. (2017) and Rowland et al. (2021), which removes inter-annual variability associated with discharge to isolate source-driven concentration trends. In contrast, our analysis explicitly retains discharge variability to capture realized riverine loads and its coupling with nitrogen surplus. This approach preserves the influence of long-term changes in flow magnitude and variability driven by climate, land use, and water management.

2.3. Watershed Nitrogen Inputs and Outputs

We used the Gridded TRajEctories Nutrient Data set for Nitrogen (gTREND-Nitrogen), which is an 88-year 250 m gridded data set of annual nitrogen inputs and outputs by Chang et al. (2025, 2026). The data set includes the following annual fluxes: atmospheric nitrogen deposition (kg-N ha^{-1} y^{-1}), inorganic nitrogen fertilizer (kg-N ha^{-1} y^{-1}), biological nitrogen fixation (kg-N ha^{-1} y^{-1}), nitrogen in livestock manure (kg-N ha^{-1} y^{-1}), crop and pasture nitrogen uptake (kg-N ha^{-1} y^{-1}), and nitrogen in human waste (kg-N ha^{-1} y^{-1}). Annual nitrogen surplus is calculated as the difference between anthropogenic nitrogen inputs and non-hydrological outputs (crop and pastureland nitrogen uptake). The gridded inputs were aggregated to the watershed scale by taking the mean value for each watershed for a given year using zonal statistics from the rasterstats package in Python (Perry, 2023).

2.4. Trend Analysis and Quadrant Classification

We estimated trends in nitrogen surplus and riverine loads in individual watersheds from 1990 to 2017 unless the available data ended earlier, in which case we used whatever endpoint was available. We used the Mann-Kendall non-parametric test for monotonic trend (Helsel et al., 2020). We implemented a variance correction to address autocorrelation, which was detected in 36% of loads and 86% of nitrogen surplus time series, improving the accuracy of the Mann-Kendall test (Millard, 2013; Patakamuri & O'Brien, 2021). The variance correction method developed by Yue and Wang (2004) first removes any trend from the data, and then it estimates the serial correlation among the detrended data points. Afterward, it employs the concept of effective sample size to adjust for the impact of this estimated serial correlation on statistical tests or analyses. We then used the Theil-Sen slope to quantify the rate of change (Patakamuri & O'Brien, 2021), and normalized it by the mean of the time series to express it as annual percentage change.

We then categorized each watershed with a significant ($\alpha = 0.1$) trend in both nitrogen surplus and riverine loads into four quadrants based on the direction of change in both variables, adapting a framework applied to phosphorus loads by Stackpoole et al. (2019). Watersheds with increasing nitrogen surplus and loads are classified as input-driven watersheds (Q1); decreasing in surplus and increasing in loads as transitioning watersheds (Q2); decreasing nitrogen surplus and loads as bright spot watersheds (Q3); and increasing surplus and decreasing loads as delayed-response watersheds (Q4).

2.5. Watershed Characteristics

We compiled watershed characteristics from multiple sources to characterize land use, climate, soil properties, and land management practices across watersheds. Watershed areas, average baseflow index (BFI; %), 2010 block-level population density, and land use were obtained from Falcone (2017), which was generated for studies being performed as part of the Surface Water Trends project, USGS National Water Quality Program (Murphy, 2020; Oelsner & Stets, 2019; Sprague et al., 2019; Stackpoole et al., 2021). Baseflow index is a static long-term estimate and does not account for changes in baseflow from landscape modifications (Wolock, 2003). We derived a "natural land use" category aimed at capturing low-impact land uses, by summing wetland, open water, forested, shrubland, grassland, and barren land use. Aridity index (AI as Evapotranspiration/Precipitation) data was obtained from CGIAR Global Aridity Index data set averaged over 1970–2000 (Zomer & Trabucco, 2022).

To determine the extent of the watersheds' agricultural land that is tile-drained, we performed a two-step process. First, we used a 30-m resolution data set of tile-drained areas to calculate the percent of the watershed that is tile-drained (Valayamkunnath et al., 2020). Next, we divided the percent of the watershed that is tile-drained by

23284277, 2026, 8, Downloaded from https://agupubs.onlinelibrary.wiley.com/doi/10.1029/2026EF008532, Wiley Online Library on [03/11/2026]. See the Terms and Conditions (https://onlinelibrary.wiley.com/terms-and-conditions) on Wiley Online Library for rules of use; OA articles are governed by the applicable Creative Commons License

percent agricultural land to determine the percent of agricultural land that is tile-drained, referred to as "percent tile-drained area."

To characterize livestock agriculture, we used 5 arc min 2015 livestock density data set (Gilbert et al., 2018), which spatially distributed livestock densities based on environmental predictors. For each watershed, we calculated livestock density by first summing the gridded densities for cattle, chicken, goats, horses, pigs, and sheep within each grid cell, then computing the mean across all grid cells within the watershed boundary. Livestock density was log-transformed for analysis (log km^{-2}) but reported as heads per km^{-2}.

Soil water pH, percent clay, and percent silt were obtained from the Probabilistic Remapping of SSURGO (POLARIS) data set at the 30-m resolution (Chaney et al., 2019). POLARIS soil properties were aggregated to 0–200 cm depth using depth-weighted means. We summed percent clay and percent silt into a single fine-texture soil fraction (percent clay and silt) because individually they are highly correlated and exhibit low hydraulic conductivity relative to sand.

We calculated several indices to characterize watershed nitrogen dynamics and agricultural management. The export ratio (E_r) was calculated as the ratio of average riverine load to average nitrogen surplus (2003–2017 or to the end of each time series, whichever was more recent), to represent the fraction of a watershed's contemporary nitrogen surplus loss through riverine export. Mean atmospheric nitrogen deposition (kg-N ha^{-1} yr^{-1}) was calculated by averaging the values from our gTReEND-Nitrogen data set over the same period.

2.6. Machine Learning Classification Model and SHAP Analysis

We used a machine learning model with SHAP (SHapley Additive exPlanations) values to identify which watershed characteristics were most associated with quadrant membership and how they influence classification (Lundberg et al., 2020; Lundberg & Lee, 2017). We then complemented this analysis with descriptive statistics to contextualize these patterns.

2.6.1. Model Development

We used an eXtreme Gradient Boosting (XGB) multiclass model to predict watersheds' classification in the four quadrants. Ensemble tree multiclass models are known for their strong performance in similar classification studies and can capture complex interactions despite the noisy, nonlinear, and intercorrelated nature of environmental data (Hastie et al., 2009; Tesoriero et al., 2024; Yuan et al., 2025; Q. Zhang et al., 2022). XGB specifically has a built-in L2 regularization, which helps prevent overfitting given our relatively small sample size (Chen & Guestrin, 2016; Friedman, 2001). We implemented the model using the Python package "xgboost" (XGBoost Python Package — xgboost 0.90 documentation, n.d.).

The model was trained on the complete data set (all 281 watersheds with significant trends in both surplus and riverine loads) to maximize the stability of the learned associations. Hyperparameters were tuned using 5-fold cross validation across 1620 combinations, selecting the parameter set with the highest weighted F1 score. To evaluate the model performance without a separate holdout set, we used a bootstrap out-of-bag (OOB) resampling, an approach that provides performance estimates while maximizing the training data available (Efron, 1983; Hastie et al., 2009). We generated 200 bootstrapped training sets by sampling watersheds with replacement from the original data set. The model was fitted to this bootstrap sample using identical hyperparameters, and performance was evaluated on OOB samples not included in the bootstrapped sample set. This approach provides a nearly unbiased estimate of model performance using independent data sets while allowing the final model to be trained on the complete data set. We report the aggregated model performance by taking the mean across all 200 runs.

2.6.2. Predictors Selection and SHAP Analysis

The predictors used in the model were selected through a multi-step, iterative process. We initially compiled a set of approximately 100 variables, which were filtered based on correlation analysis. Predictors with a Spearman correlation coefficient over 0.6 were flagged, and we chose between predictors with greater interpretability based on domain knowledge. In some cases, high correlations reflect regional co-occurrence rather than mechanistic redundancy. For example, agricultural land use and tile drainage are highly correlated in the Midwest but vary

23284277, 2026, 8, Downloaded from https://agupubs.onlinelibrary.wiley.com/doi/10.1029/2026EF008532, Wiley Online Library on [03/11/2026]. See the Terms and Conditions (https://onlinelibrary.wiley.com/terms-and-conditions) on Wiley Online Library for rules of use; OA articles are governed by the applicable Creative Commons License

independently in other regions (see Figure S2 in Supporting Information S1 for final correlation matrix). In these cases, we retained both to preserve characteristics that may distinguish behavior in different regions.

After removing correlated watershed characteristics, the remaining 24 predictors were evaluated based on their influence on the model. We used SHAP values to determine the predictors with the largest influence on the model classification (Lundberg et al., 2020; Lundberg & Lee, 2017). SHAP values quantify each characteristics' contribution to the model's prediction for each watershed for each class. In multiclass problems, each characteristic has m SHAP numbers corresponding to each class. Each SHAP value represents the characteristic's contribution to the log-odds of each class. A positive SHAP value pushes the prediction toward that class, whereas a negative value pushes away from it. Larger magnitude indicates a stronger influence. In multiclass problems, understanding a characteristic's influence on a class requires analyzing SHAP values relative to other classes' SHAP values because a characteristic that pushes strongly toward one class pushes away from others. We therefore analyze each quadrant's SHAP values and identify characteristics with large positive or negative values diagnostic of that quadrant's behavior, relative to the others' SHAP values.

We iteratively reduced the watershed characteristic set from 24 to 12 to balance parsimony and interpretability. Characteristics were removed if they were consistently ranked low in mean absolute SHAP across all quadrants, were conceptually redundant with higher-ranking characteristics, or could be removed without impacting model performance. To assess the stability of SHAP values in the final model, we trained 10 models using identical hyperparameters but different random seeds, computed SHAP values for each, and aggregated results across runs. We report mean absolute SHAP values magnitudes with standard deviations (Figure S3 in Supporting Information S1).

2.6.3. Quadrant Descriptive Statistical Analysis

We complemented the SHAP analysis with the use of descriptive statistics to interpret the patterns driving classification and explore watershed characteristics that are associated with each input-load response quadrant. We compared characteristics representing land use (agricultural, grassland, and natural land use), nitrogen sources and management (net agricultural nitrogen inputs, livestock density, atmospheric deposition, and population density), hydrology and climate (percent tile-drained area, BFI, export ratio, and aridity index), and soil properties (pH and clay and silt content). We compared the 12 model characteristics plus three additional characteristics: net agricultural nitrogen inputs, grassland land use, and export ratio, which were not included as characteristics in the model. We used the Wilcoxon rank-sum test to determine whether the distributions of these characteristics differed significantly between quadrants (Helsel et al., 2020).

3. Results and Discussion

3.1. Temporal Trends in Nitrogen Surplus and Riverine Loads

Exploring trends over the last 30 years, we find nitrogen surplus to be significantly decreasing ($p < 0.1$) in 53% of the study watersheds (median rate: −1.32% per year; range: −8.87% to −0.07% per year) and increasing ($p < 0.1$) in 31% of the watersheds (median rate: 1.25% per year; range: 0.08%–6.81% per year), while there is no significant change in 16% of the watersheds (Figures 1a–1d). Watersheds with increasing nitrogen surplus are concentrated in the interior US, including the Mississippi River Basin and Missouri River Basin, and a few western watersheds, including the Columbia River Basin. On the other hand, watersheds with decreasing nitrogen surplus are found in the eastern US, Florida, and eastern Mississippi River Basin tributaries.

Riverine nitrogen load trends over the same time frame (1990–2017) follow similar patterns, but with fewer decreasing and more insignificant trends. Specifically, we find decreasing ($p < 0.1$) trends in 39% of the watersheds (median rate: −1.86% per year; range: −13.0% to −0.25% per year) and increasing trends ($p < 0.1$) in 30% of watersheds (median rate = 1.90% per year; range: 0.27%–8.11% per year), while 32% of the watersheds exhibited no significant trend (Figures 1e–1h). Watersheds with increasing loads are in Florida, the Mississippi River basin and the Missouri River Basin, while watersheds with decreasing loads are concentrated in the eastern US and watersheds in Oklahoma and Kansas. The greater proportion of decreasing trends in nitrogen surplus compared to decreases in nitrogen loads suggests that input reductions are not always accompanied by significant declines in loads, highlighting the role of watersheds in temporarily storing past nitrogen inputs and releasing them over time through legacy effects (Basu et al., 2011).

10.1029/2026EF008532

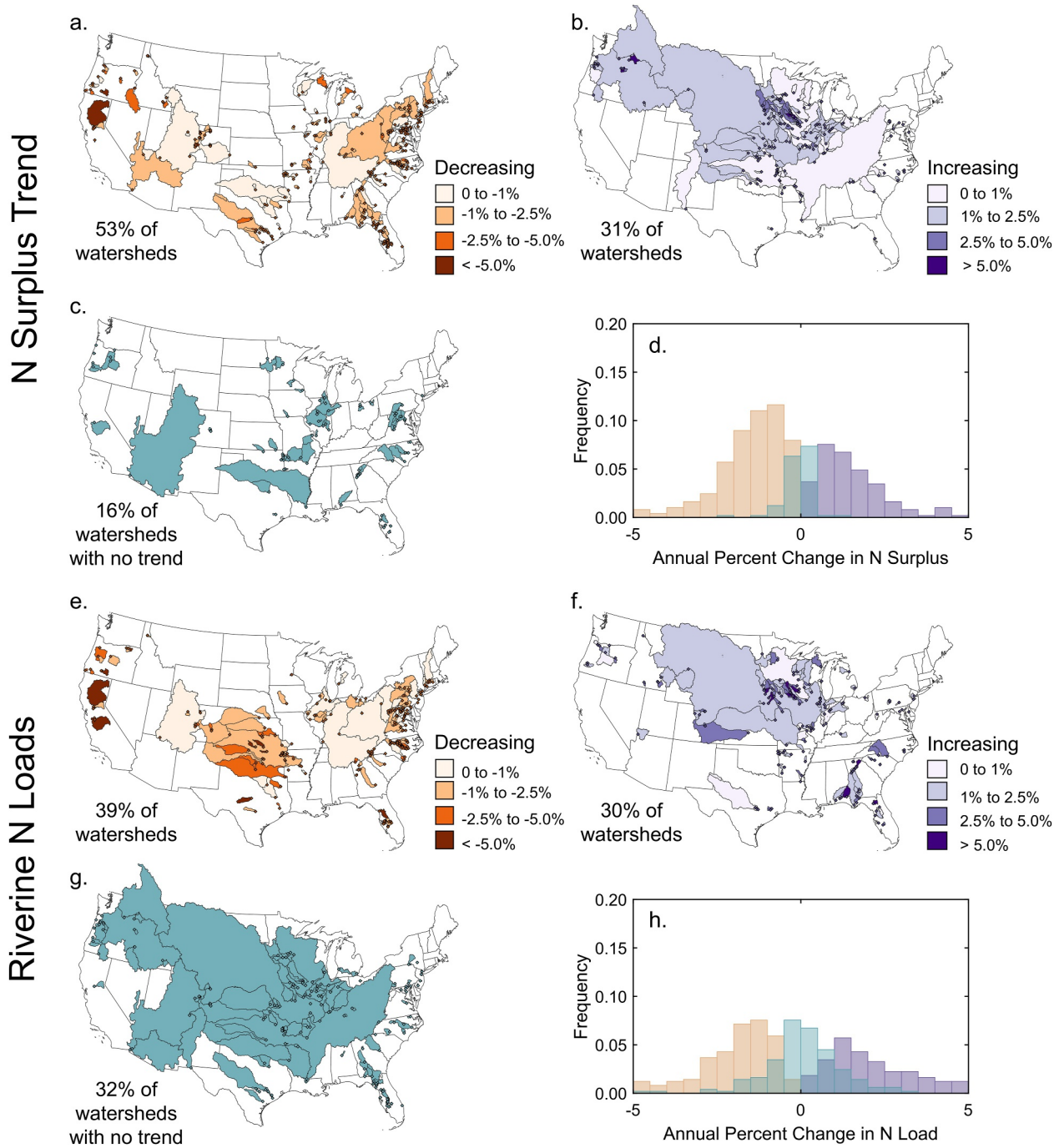


Figure 1. Watershed trends in nitrogen surplus (a–d) and loads (e–h) over the last three decades (1990–2017). Panels (a–c) watersheds with decreasing, increasing ($p \leq 0.1$), and no significant trend ($p > 0.1$) in nitrogen surplus; (d) histogram of the annual percent change in nitrogen surplus; (e–g) watersheds with decreasing, increasing ($p \leq 0.1$), and no significant trend ($p > 0.1$) in riverine nitrogen loads; (h) histogram of the annual percent change in loads.

Trends in nitrogen surplus are partly a function of land use and management trajectories that determine nitrogen inputs, and thus are shaped by broader scale socio-economic and environmental factors. These factors include shifts in crop demand and market, such as those that coincided with expanded corn production for biofuels (Donner & Kucharik, 2008; Lark et al., 2022), changes in atmospheric deposition associated with air quality regulations (Byrnes et al., 2020; Lloret & Valiela, 2016), increased concentration of livestock operations (Byrnes et al., 2020; Glibert, 2020), and increases in crop yield, and improvements in nitrogen use efficiency (Swaney

23284277, 2026, 8, Downloaded from https://agupubs.onlinelibrary.wiley.com/doi/10.1029/2026EF008532, Wiley Online Library on [03/11/2026]. See the Terms and Conditions (https://onlinelibrary.wiley.com/terms-and-conditions) on Wiley Online Library for rules of use; OA articles are governed by the applicable Creative Commons License

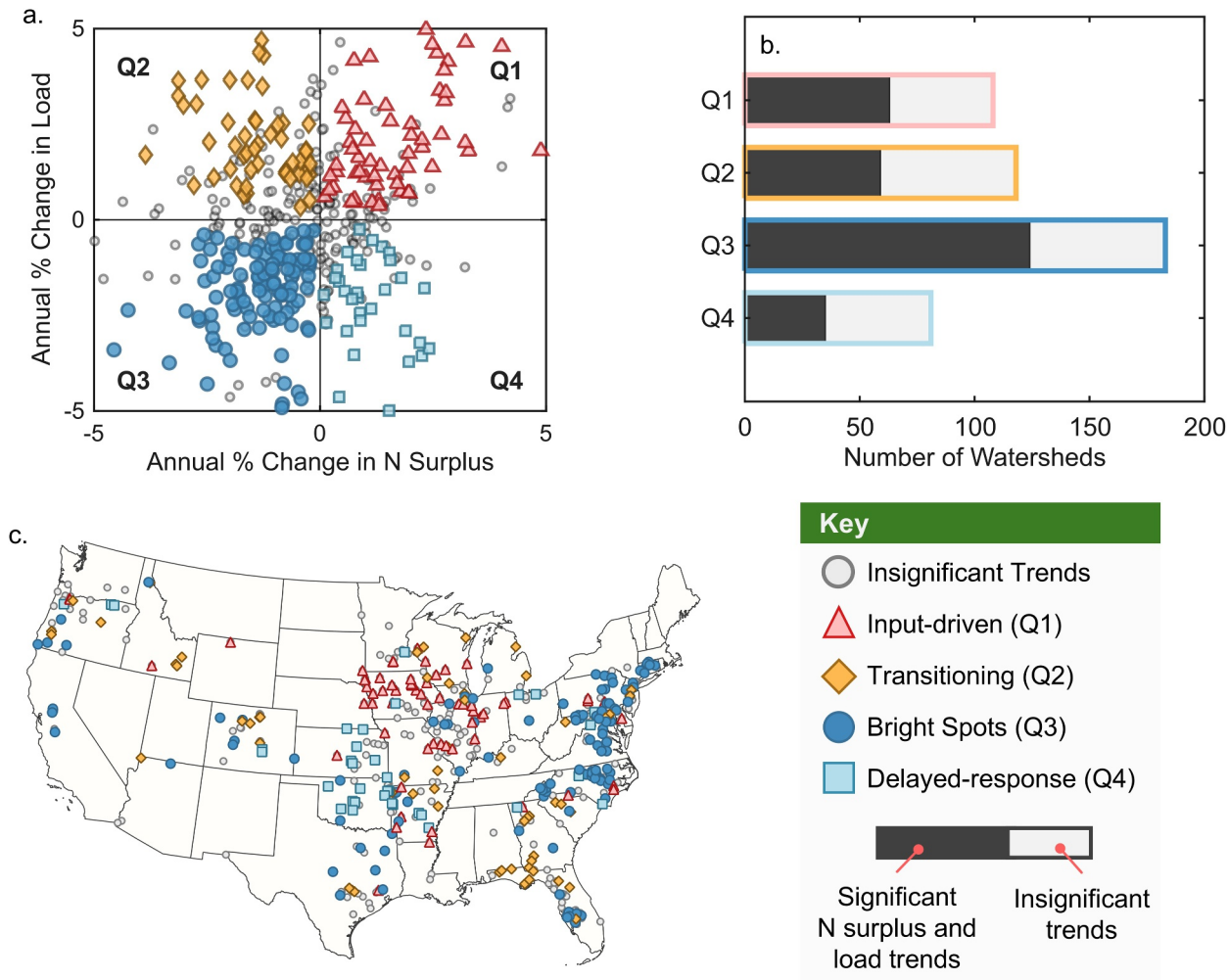


Figure 2. Relationship between annual percent change of nitrogen surplus and riverine loads. (a) Quadrant plot of the four typologies of watershed response: input-driven quadrant (Q1) with increases in both nitrogen surplus and loads; transitioning quadrant (Q2) with decreases in nitrogen surplus and increases in loads; bright spots quadrant (Q3) with decreases in both nitrogen surplus and loads; delayed-response quadrant (Q4) with increases in nitrogen surplus and decreases in loads. (b) The distribution of significant and insignificant watersheds in each quadrant ($p < 0.1$) in both nitrogen surplus and loads. (c) Spatial distribution of the four quadrants, highlighting the geographical variation in watershed response.

et al., 2018). Trends in riverine nitrogen loads, on the other hand, reflect the combined influence of both current and past nitrogen surplus, as well as landscape, soil, and climate attributes that determine how nitrogen is being processed and transported through the landscape. These landscape factors that modulate nitrogen surplus contribute to a larger proportion of the watersheds showing no significant trend in nitrogen loads, despite a decreasing or increasing trend in nitrogen surplus.

3.2. Typologies of Watershed Responses to Nitrogen Dynamics

We further explored the relationship between nitrogen surplus and riverine load trends by grouping watersheds according to the joint direction of their trends. This grouping reveals that watersheds span a range of behaviors, from systems where surplus and load trends are in the same direction to systems where they are in opposite directions. The analysis revealed four distinct response typologies (Figure 2a): (a) input-driven watersheds (Q1; 108 total, of which 63 have significant trends), where both surplus and load are increasing; (b) transitioning watersheds (Q2; 118 total, 59 significant), where surplus is decreasing while load is increasing; (c) bright spot watersheds (Q3; 183 total, 124 significant) where both nitrogen surplus and load are decreasing; and (d) delayed-response watersheds (Q4; 81 total, 35 significant) where surplus is increasing while load is decreasing.

23284277, 2026, 8, Downloaded from https://agupubs.onlinelibrary.wiley.com/doi/10.1029/2026EF008532, Wiley Online Library on [03/11/2026]. See the Terms and Conditions (https://onlinelibrary.wiley.com/terms-and-conditions) on Wiley Online Library for rules of use; OA articles are governed by the applicable Creative Commons License

10.1029/2026EF008532

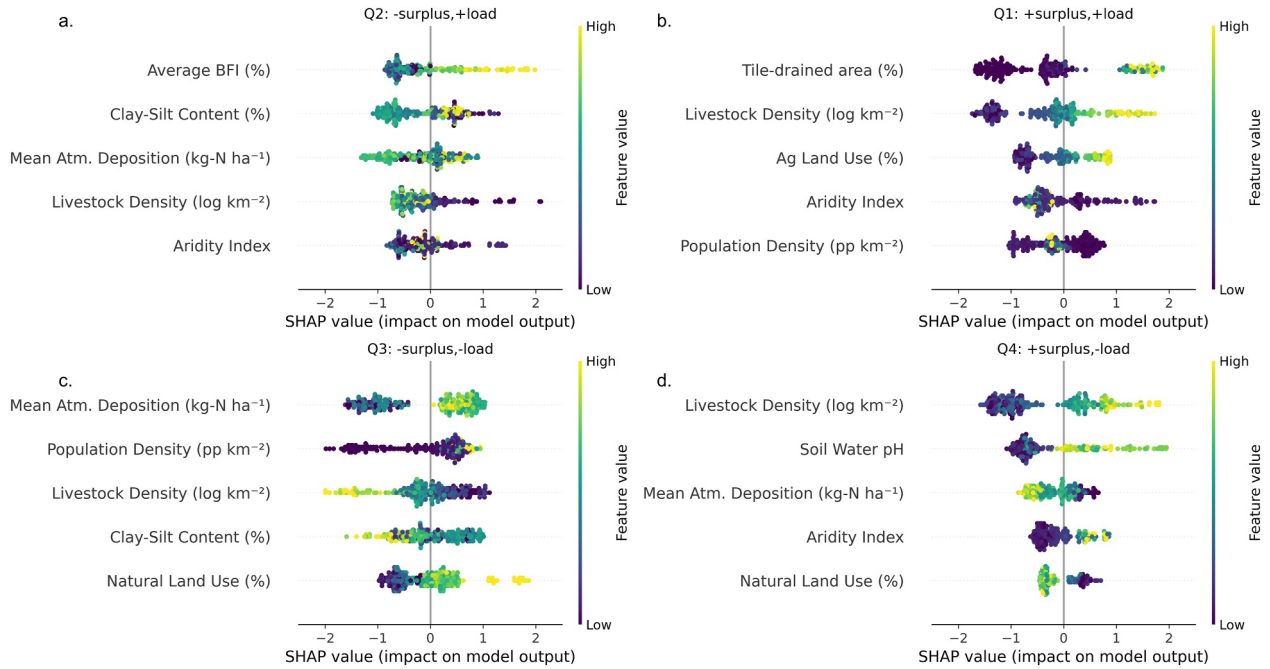


Figure 3. SHAP beeswarm plot for top five characteristics for each quadrant. Positive SHAP values pushes classification toward that quadrant, whereas negative SHAP values pushes classification away from the quadrant. Figure S4 in Supporting Information S1 contains SHAP values for all characteristics.

The classification of watersheds into quadrants depends on the direction of estimated surplus and load trends. Uncertainty in the underlying data in both nitrogen inputs and riverine loads can influence the classification, particularly in watersheds with weak or marginal trends, which are most sensitive to uncertainty. The nitrogen surplus data set is compiled from multiple estimated components, each with its own uncertainty arising from the underlying data and the methods used to harmonize them. These sources are described in detail in Chang et al. (2026). For riverine loads, we estimate trends using actual rather than flow-normalized loads, consistent with our focus on realized nitrogen export to receiving waters. Since loads are largely governed by discharge, trend estimates from actual loads can be sensitive to hydrological conditions at the end of the record. Wet or dry years can generate trends that reflect discharge variability rather than a change in the watershed's nitrogen dynamics (Q. Zhang et al., 2026). While quantifying these uncertainties is outside of the scope of this work, periodic updates to this analysis can ensure results reflect our most current data and that updated information is communicated to decision-makers.

To explore which watershed characteristics are most strongly associated with each response typology, we used an XGB classifier as an exploratory, multivariate tool. Model performance indicated moderate separability among response types (mean F1 score across 200 bootstrap iterations: 0.65 ± 0.04), with the strongest performance for bright spot watersheds (Q3; mean F1 = 0.73) and the weakest for transitioning watersheds (Q2; mean F1 = 0.49). This variation reflects differences in coherence among response types, with transitional systems exhibiting greater heterogeneity. Because our objective is interpretation rather than prediction, we use the model to identify characteristics associated with each response type rather than to assign watershed membership. Statistical pairwise comparisons between watershed characteristics are reported in Table S1 in Supporting Information S1.

3.2.1. Input-Driven Watersheds (Q1)

Of the 63 input-driven watersheds with significant increases in both surplus and load (Q1), 45 are located in the Midwestern states (Figure 2c). SHAP analysis highlights a clear and coherent signature for this group (Figure 3b). Tile-drained area emerges as the dominant distinguishing characteristic, with values exceeding ~20% of agricultural land strongly pushing watersheds toward Q1 classification (Figure S4 in Supporting Information S1). Livestock density and agricultural land use also exert strong positive influence, with higher values of both variables increasing the likelihood of Q1 membership (Figure S4 in Supporting Information S1).

23284277, 2026, 8, Downloaded from https://agupubs.onlinelibrary.wiley.com/doi/10.1029/2026EF008532, Wiley Online Library on [03/11/2026]. See the Terms and Conditions (https://onlinelibrary.wiley.com/terms-and-conditions) on Wiley Online Library for rules of use; OA articles are governed by the applicable Creative Commons License

23284277, 2026, 8, Downloaded from https://agupubs.onlinelibrary.wiley.com/doi/10.1029/2026EF008532, Wiley Online Library on [03/11/2026]. See the Terms and Conditions (https://onlinelibrary.wiley.com/terms-and-conditions) on Wiley Online Library for rules of use; OA articles are governed by the applicable Creative Commons License

These SHAP patterns are reflected in the descriptive characteristics of Q1 watersheds, which exhibit extensive tile drainage (median 30% of agricultural land, compared to <1% in all other quadrants), high agricultural land use (median 68.7%), and high livestock density (median 200 heads km^{-2}) (Figures 4b–4d). Together, these characteristics correspond to the highest net agricultural nitrogen inputs (median: 49.1 kg-N ha^{-1} yr^{-1}; Figure 4e) and export ratios (median: 0.18) among all response types, indicating strong coupling between nitrogen inputs and riverine load.

The combination of high nitrogen inputs and extensive tile drainage creates conditions for rapid nitrogen transport from fields to streams, reducing subsurface travel times and limiting opportunities for denitrification. Previous studies have shown that tile drainage can contribute the majority of nitrogen export in such systems by enhancing hydrologic connectivity (Liu et al., 2021; Schilling et al., 2020; Zhao et al., 2025). These are therefore short-memory systems, where riverine loads are tightly coupled to current inputs rather than the legacy of past inputs. Consequently, we consider them "opportunity spots" where reductions in fertilizer application, improvements in nitrogen use efficiency, and enhanced livestock management could yield relatively rapid water-quality benefits.

3.2.2. Transitioning Watersheds (Q2)

Transitioning watersheds (Q2) exhibit a decoupled response, with declining nitrogen surplus but increasing riverine load. These watersheds are distributed across the United States, with some clustering in the southeastern region (Figures 2b and 2c). SHAP analysis identifies BFI as the most influential characteristic distinguishing Q2 watersheds, with higher BFI consistently pushing watersheds toward Q2 classification (Figure 3a). This effect is strong and monotonic, indicating a dominant role of groundwater-dominated hydrology in shaping this response type.

Several additional characteristics, clay-silt content, atmospheric nitrogen deposition, and livestock density, exhibit comparable mean absolute SHAP values, indicating that they contribute similarly to the model's ability to distinguish Q2 watersheds (Figure 3a). However, SHAP dependence plots reveal important differences in how these variables influence classification. Livestock density shows a clear and largely monotonic relationship, with increasing livestock density consistently pushing watersheds away from Q2 membership (Figure S4 in Supporting Information S1), reinforcing the association of Q2 with low contemporary agricultural pressure. In contrast, clay-silt content and atmospheric deposition exhibit non-monotonic and threshold-dependent responses, with their influence varying across the range of values and depending on interactions with other watershed characteristics.

These patterns are reflected in the descriptive characteristics of Q2 watersheds, which are characterized by high BFI (median: 54%, Figure 4i), low livestock density (median: 25 km^{-2}; Figure 4c), low agricultural land use (median: 14.4%; Figure 4b), low net agricultural inputs (median: 6.2 kg-N ha^{-1} yr^{-1}; Figure 4e), and high natural land cover (median: 70%; Figure 4l). Together, these characteristics point to systems where riverine nitrogen loads are primarily sustained by slow release of legacy nitrogen through groundwater pathways rather than by current nitrogen inputs.

This interpretation is consistent with previous studies linking elevated BFI to groundwater-derived nitrate fluxes and long response lags in water quality (Ascott et al., 2017; Basu et al., 2022; Chang et al., 2021; Johnson & Stets, 2020; Van Meter et al., 2023; Vero et al., 2017). As legacy stores are gradually depleted, these watersheds may eventually transition toward the bright spot response (Q3), although the timing of such recovery remains uncertain.

3.2.3. Bright Spot Watersheds (Q3)

Bright spot watersheds (Q3) form the largest response group, comprising 124 watersheds with statistically significant declines in both nitrogen surplus and load. These watersheds are concentrated primarily in the northeastern US (Figure 2c). SHAP analysis identifies a coherent signature distinguishing these systems, with atmospheric deposition, population density, livestock density, clay-silt content and natural land use emerging as the most influential characteristics (Figure 3c).

Higher population density and atmospheric deposition exert a positive influence on Q3 classification, while higher livestock density pushes watersheds away from this response type. In particular, population density

10.1029/2026EF008532

23284277, 2026, 8, Downloaded from https://agupubs.onlinelibrary.wiley.com/doi/10.1029/2026EF008532, Wiley Online Library on [03/11/2026]. See the Terms and Conditions (https://onlinelibrary.wiley.com/terms-and-conditions) on Wiley Online Library for rules of use; OA articles are governed by the applicable Creative Commons License

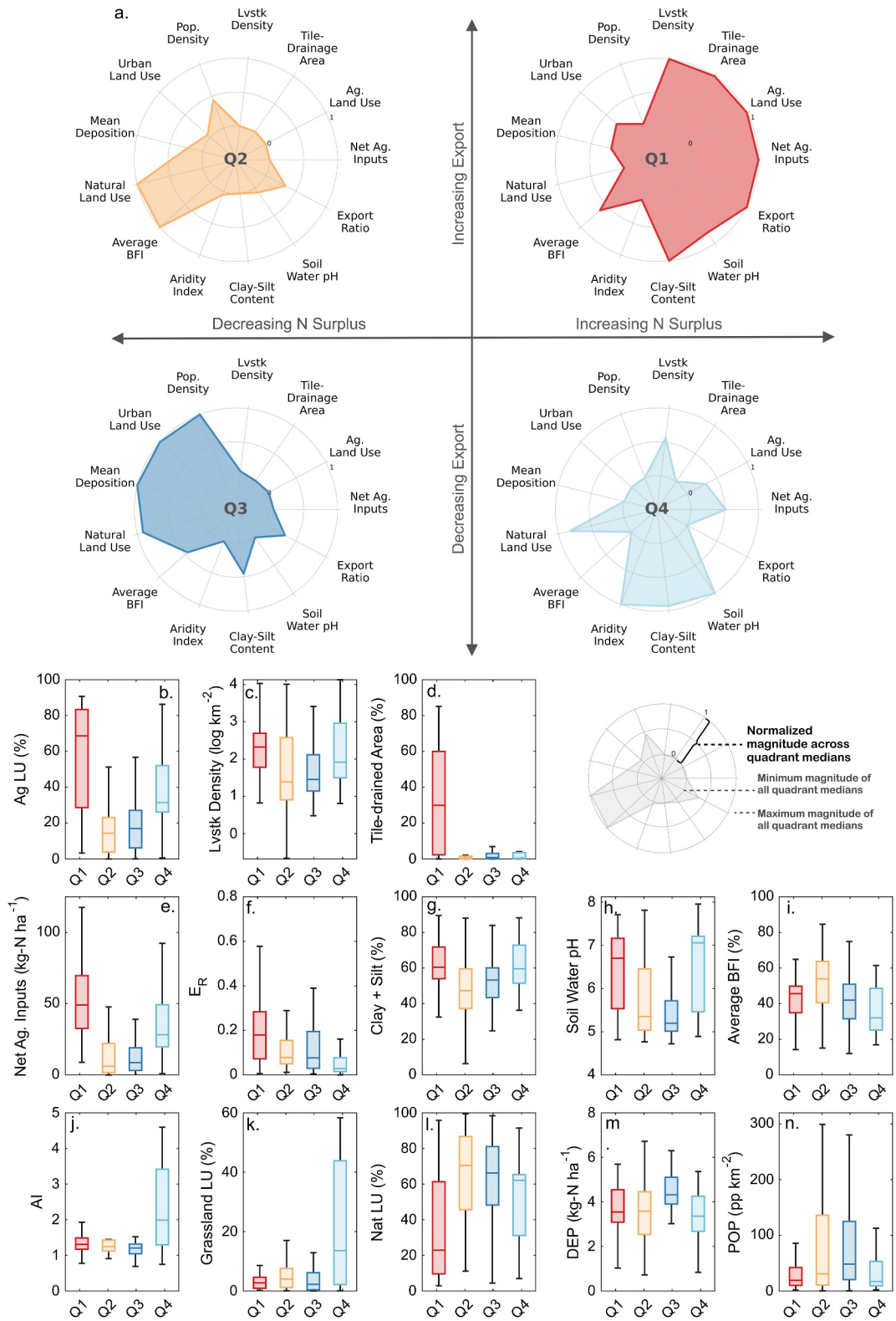


Figure 4. Comparison of the distributions of watershed characteristics across quadrants. (a) Spider plot capturing the median characteristics of watersheds in each quadrant, normalized using min-max normalization of the median values. (b–n) are the distribution of quadrant characteristics for each quadrant. The spider plots display ranges from the inner (minimum) to the outer (maximum) median magnitudes for specific characteristics across the quadrants.

23284277, 2026, 8, Downloaded from https://agupubs.onlinelibrary.wiley.com/doi/10.1029/2026EF008532, Wiley Online Library on [03/11/2026]. See the Terms and Conditions (https://onlinelibrary.wiley.com/terms-and-conditions) on Wiley Online Library for rules of use; OA articles are governed by the applicable Creative Commons License

exceeding ~20 persons km^{-2}, natural land use exceeding ~60%, atmospheric deposition exceeding 4 kg-N ha^{-1}, and livestock density below ~2 log km^{-2} are all associated with Q3 membership (Figure 3c and Figure S4 in Supporting Information S1). In contrast, clay-silt content, while ranked similarly by SHAP, shows a weak and non-monotonic relationship, with no clear threshold or directional relationship across its range. This suggests that clay-silt content contributes to classification primarily through interactions with other watershed characteristics rather than acting as a primary mechanistic control in these systems.

These SHAP patterns are consistent with the descriptive characteristics of Q3 watersheds, which are characterized by low agricultural land use (median: 17%; Figure 4b), low livestock density (median: 28 heads km^{-2}; Figure 4c), high natural land use (median: 66.2%; Figure 4l), and elevated population density (median: 48.2 pp km^{-2}; Figure 4n). Q3 watersheds also experience the highest atmospheric deposition rates among quadrants (median: 4.3 kg-N ha^{-1} yr^{-1}; Figure 4m), consistent with their concentration in the northeastern US (Figure 2c), where long-term declines in atmospheric nitrogen deposition have been documented.

Together, these characteristics point to watersheds with low contemporary agricultural pressure, strong urban influence, and effective source controls, where reductions in nitrogen inputs have translated into measurable improvements in water quality. Decreasing nitrogen loads in Q3 likely reflect the combined effects of already-low agricultural inputs, sustained reductions in atmospheric deposition, and improvements in wastewater treatment and urban nutrient management (Chang et al., 2021; Harding et al., 2019; Lefcheck et al., 2018; Oelsner & Stets, 2019; Stets et al., 2020). Consistent with the role of atmospheric deposition, work in the Chesapeake Bay found that reductions in nitrate loads across many subwatersheds could be attributed to reductions in atmospheric deposition following air quality regulations (Chang et al., 2021; Eshleman & Sabo, 2016). These systems provide empirical evidence that coordinated policy interventions can produce detectable water-quality improvements at the watershed scale.

3.2.4. Delayed-Response Watersheds (Q4)

Delayed-response watersheds (Q4) comprise 35 watersheds in which nitrogen load is decreasing despite increasing nitrogen surplus and are primarily clustered in the central United States (Figure 2c). SHAP analysis indicates that these watersheds are characterized by a strong nitrogen input signal associated with livestock density, alongside climate and transport constraints captured by aridity index and related soil properties (Figure 3d).

Livestock density emerges as the dominant input-related characteristic, with SHAP values becoming strongly positive above approximately 2 log km^{-2}. This threshold mirrors that observed for input-driven watersheds (Q1), indicating that high livestock production is a dominant driver of increasing nitrogen surplus across both response types. SHAP dependence plots reinforce this interpretation (Figure S4 in Supporting Information S1), showing that increasing livestock density consistently pushes watersheds toward higher surplus states. Consistent with this pattern, Q4 watersheds exhibit relatively high livestock density (median: 79 heads km^{-2}; Figure 4c) and moderately elevated net agricultural nitrogen inputs (median: 28.3 kg-N ha^{-1} yr^{-1}; Figure 4e). However, unlike Q1, these inputs occur in landscapes with limited hydrologic connectivity. Q4 watersheds have very low tile drainage extent (median: 0.37%; Figure 4d) and substantially lower export ratios than all other quadrants (median: 0.03), indicating weak coupling between surplus and riverine loads.

Climate further constrains nitrogen transport in Q4 watersheds. Aridity index shows a consistent positive association with Q4 classification, and these watersheds are significantly more arid than those in other quadrants (median: 2.0; Figure 4j). SHAP dependence plots indicate that increasing aridity suppresses nitrogen load, consistent with reduced runoff, higher evapotranspiration, and limited lateral transport. As a result, increasing nitrogen inputs do not translate into increasing riverine loads.

Soil water pH also exhibits a generally positive association with Q4 classification, though its relationship is more variable and non-linear. Rather than acting as an independent control on nitrate loads, elevated pH in Q4 likely reflects the same arid and semi-arid conditions that limit leaching and promote base-cation accumulation. This is consistent with the observation that Q4 watersheds exhibit the highest median soil water pH among quadrants (median: 7.1; Figure 4h). The similar directional behavior of soil pH and aridity in the SHAP dependence plots suggests that pH serves primarily as an indicator of climatic and hydrologic setting rather than a mechanistic driver of nitrogen retention.

23284277, 2026, 8, Downloaded from https://agupubs.onlinelibrary.wiley.com/doi/10.1029/2026EF008532, Wiley Online Library on [03/11/2026]. See the Terms and Conditions (https://onlinelibrary.wiley.com/terms-and-conditions) on Wiley Online Library for rules of use; OA articles are governed by the applicable Creative Commons License

Taken together, Q4 watersheds represent transport-limited systems in which strong nitrogen inputs, particularly from livestock, are not yet translated into riverine loads due to arid conditions and weak hydrologic connectivity. However, declining loads may also reflect improvement in point or non-point source management, such as wastewater treatment plant upgrades or expanded agricultural best management practices, all of which reduce riverine nitrogen loads independently of surplus trajectory (Hansen et al., 2018; Sabo et al., 2022; Van Meter et al., 2023; Williams et al., 2024). Whether remaining nitrogen is being retained within the landscape or removed through biogeochemical processes remains uncertain. As surplus continues to accumulate, these watersheds may experience future increases in loads if transport pathways are activated, highlighting uncertainty in their long-term water-quality trajectories.

While these four typologies capture dominant and interpretable nitrogen response patterns, some watersheds exhibit mixed characteristics and sit near classification boundaries, reflecting additional heterogeneity not fully captured by the available predictors; these cases are explored in detail (Text S1 in Supporting Information S1).

4. Conclusion

Decades of research linking nitrogen inputs to riverine loads have set an expectation that declining inputs will translate into improved downstream water quality. Our analysis of 490 watersheds shows that water quality responses are diverse and not always proportional to changes in nitrogen surplus, with the effects of changing nitrogen surplus modulated by landscape characteristics and system history.

By jointly analyzing long-term trends in nitrogen surplus and riverine loads, we identify four distinct watershed response regimes that capture the diversity of nitrogen dynamics across the continental US: input-driven, transitioning, bright spot, and delayed-response. These regimes reveal that nitrogen load responses are governed not only by the magnitude of inputs but also by the interaction between input intensity, hydrologic connectivity, climate constraints, and legacy nitrogen storage.

Livestock density emerges as a consistent driver of increasing nitrogen surplus across both input-driven and delayed-response watersheds, reflecting the concentration of manure-derived nitrogen inputs and the spatial decoupling between production and crop nitrogen demand that characterizes modern livestock systems (Bouwman et al., 2013; Byrnes et al., 2020; Glibert, 2020). Where hydrologic connectivity is high (input driven), such as intensively tile-drained agricultural watersheds, inputs and loads remain tightly coupled, enabling relatively rapid responses to management. Where connectivity is weak, such as in arid climates with limited lateral transport (delayed-response), nitrogen loads can decline even as surplus increases, highlighting potential for legacy accumulation within the landscape.

Declining atmospheric nitrogen deposition emerges as a driver of decreasing surplus that has translated more directly into decreasing loads in bright spot watersheds with low agricultural pressure and strong urban influence. Groundwater-dominated watersheds represent a third, critically important response pathway, in which declining surplus does not immediately translate into reduced loading (transitioning watersheds) because nitrogen stored in subsurface reservoirs continues to discharge to streams over decadal timescales. Elevated baseflow contributions in these systems indicate that riverine load is sustained by groundwater transport, consistent with legacy nitrogen release documented in both empirical and modeling studies. In such watersheds, improving water quality may require not only sustained reductions in inputs, but also patience commensurate with groundwater residence times.

Taken together, our results demonstrate that spatial patterns in riverine nitrogen loads cannot be used as proxies for temporal recovery trajectories. Watersheds with high loads today are not necessarily those that will respond most rapidly to reductions in inputs, and watersheds with low or declining loads may still be accumulating nitrogen that poses future risks. Effective nitrogen management therefore requires aligning expectations and interventions with watershed-specific response regimes. Explicitly accounting for source type, transport efficiency, and legacy storage is essential for setting realistic water-quality goals, interpreting observed trends, and designing strategies that are robust to both legacy effects and future climate variability.

Conflict of Interest

The authors declare no conflicts of interest relevant to this study.

Availability Statement

The data on which this article is based are available in Byrnes et al. (2026).

Acknowledgments
The present work was financially supported by the Lake Futures Project under the Global Water Futures umbrella and provided through the Canada First Research Excellence Fund (N.B.B. and D.K.B). D.K.B. was supported by the NSERC Alexander Graham Bell Canada Graduate Scholarship. N.B.B. was supported by a Canada Research Chair appointment in Global Water Sustainability and Ecohydrology. K.J.V.M was also supported by startup funds from The Pennsylvania State University.

References

Ascott, M. J., Gooddy, D. C., Wang, L., Stuart, M. E., Lewis, M. A., Ward, R. S., & Binley, A. M. (2017). Global patterns of nitrate storage in the vadose zone. *Nature Communications*, *8*(1), 1416. https://doi.org/10.1038/s41467-017-01321-w

Basu, N. B., Thompson, S. E., & Rao, P. S. C. (2011). Hydrologic and biogeochemical functioning of intensively managed catchments: A synthesis of top-down analyses. *Water Resources Research*, *47*(10). https://doi.org/10.1029/2011wr010800

Basu, N. B., Van Meter, K. J., Byrnes, D. K., Van Cappellen, P., Brouwer, R., Jacobsen, B. H., et al. (2022). Managing nitrogen legacies to accelerate water quality improvement. *Nature Geoscience*, *15*(2), 97–105. https://doi.org/10.1038/s41561-021-00889-9

Batool, M., Sarrazin, F. J., Attinger, S., Basu, N. B., Van Meter, K. J., & Kumar, R. (2022). Long-term annual soil nitrogen surplus across Europe (1850–2019). *Scientific Data*, *9*(1), 1–22. https://doi.org/10.1038/s41597-022-01693-9

Bouraoui, F., & Grizzetti, B. (2011). Long term change of nutrient concentrations of rivers discharging in European seas. *The Science of the Total Environment*, *409*(23), 4899–4916. https://doi.org/10.1016/j.scitotenv.2011.08.015

Bouwman, L., Goldewijk, K. K., Van Der Hoek, K. W., Beusen, A. H. W., Van Vuuren, D. P., Willems, J., et al. (2013). Exploring global changes in nitrogen and phosphorus cycles in agriculture induced by livestock production over the 1900–2050 period. *Proceedings of the National Academy of Sciences of the United States of America*, *110*(52), 20882–20887. https://doi.org/10.1073/pnas.1012878108

Boyer, E. W., Goodale, C. L., Jaworski, N. A., & Howarth, R. W. (2002). Anthropogenic nitrogen sources and relationships to riverine nitrogen export in the northeastern U.S.A. *Biogeochemistry*, *57*(1), 137–169. https://doi.org/10.1023/A:1015709302073

Byrnes, D. K., Van Meter, K. J., & Basu, N. B. (2020). Long-term shifts in U.S. nitrogen sources and sinks revealed by the new TREND-nitrogen data set (1930–2017). *Global Biogeochemical Cycles*, *34*(9), e2020GB006626. https://doi.org/10.1029/2020GB006626

Byrnes, D. K., Van Meter, K. J., & Basu, N. B. (2026). Data release: Nitrogen memoryscapes: Typologies of nitrogen inputs and riverine loads across the Continental United States (version 1) [Dataset]. *Figshare*. https://doi.org/10.6084/m9.figshare.25998349

Chaney, N. W., Minasny, B., Herman, J. D., Nauman, T. W., Brungard, C. W., Morgan, C. L. S., et al. (2019). POLARIS soil properties: 30-m probabilistic maps of soil properties over the contiguous United States. *Water Resources Research*, *55*(4), 2916–2938. https://doi.org/10.1029/2018WR022797

Chang, S. Y., Byrnes, D. K., Basu, N. B., & Van Meter, K. J. (2026). gTREND-Nitrogen - Long-Term nitrogen mass balance data for the contiguous United States (1930-2017). *Scientific Data*, *13*(1), 562. https://doi.org/10.1038/s41597-026-06576-x

Chang, S. Y., Byrnes, D. K., Van Meter, K., & Basu, N. B. (2025). gTREND-Nitrogen - Long-Term nitrogen mass balance data for the contiguous United States (1930-2017) [Dataset]. *figshare*. https://doi.org/10.6084/m9.figshare.29897375

Chang, S. Y., Zhang, Q., Byrnes, D. K., Basu, N. B., & Van Meter, K. J. (2021). Chesapeake legacies: The importance of legacy nitrogen to improving Chesapeake Bay water quality. *Environmental Research Letters*, *16*(8), 085002. https://doi.org/10.1088/1748-9326/ac0d7b

Chen, T., & Guestrin, C. (2016). XGBoost: A scalable tree boosting system. *Proceedings of the 22nd ACM SIGKDD International Conference on Knowledge Discovery and Data Mining*, 785–794. https://doi.org/10.1145/2939672.2939785

DeCicco, L., Hirsch, R. M., Lorenz, D., Watkins, D., & Johnson, M. (2021). dataRetrieval: R packages for discovering and retrieving water data available from U.S. federal hydrologic web services (v.2.7.7). *U.S. Geological Survey*. https://doi.org/10.5066/P9X4L3GE

Díaz, R. J., & Rosenberg, R. (2011). Introduction to environmental and economic consequences of hypoxia. *International Journal of Water Resources Development*, *27*(1), 71–82. https://doi.org/10.1080/07900627.2010.531379

Donner, S. D., & Kucharik, C. J. (2008). Corn-based ethanol production compromises goal of reducing nitrogen export by the Mississippi River. *Proceedings of the National Academy of Sciences of the United States of America*, *105*(11), 4513–4518. https://doi.org/10.1073/pnas.0708300105

Dupas, R., Minaudo, C., Gruau, G., Ruiz, L., & Gascuel-Odoux, C. (2018). Multidecadal trajectory of riverine nitrogen and phosphorus dynamics in rural catchments. *Water Resources Research*, *54*(8), 5327–5340. https://doi.org/10.1029/2018WR022905

Efron, B. (1983). Estimating the error rate of a prediction rule: Improvement on cross-validation. *Journal of the American Statistical Association*, *78*(382), 316–331. https://doi.org/10.1080/01621459.1983.10477973

Ehrhardt, S., Ebeling, P., Dupas, R., Kumar, R., Fleckenstein, J. H., & Musolff, A. (2021). Nitrate transport and retention in western European catchments are shaped by hydroclimate and subsurface properties. *Water Resources Research*, *57*(10), e2020WR029469. https://doi.org/10.1029/2020wr029469

Ehrhardt, S., Kumar, R., Fleckenstein, J. H., Attinger, S., & Musolff, A. (2019). Trajectories of nitrate input and output in three nested catchments along a land use gradient. *Hydrology and Earth System Sciences*, *23*(9), 3503–3524. https://doi.org/10.5194/hess-23-3503-2019

Eshleman, K. N., & Sabo, R. D. (2016). Declining nitrate-N yields in the upper Potomac river basin: What is really driving progress under the Chesapeake Bay restoration? *Atmospheric Environment*, *146*, 280–289. https://doi.org/10.1016/j.atmosenv.2016.07.004

Falcone, J. A. (2017). Watershed characteristics for study sites of the surface water trends project [Dataset]. In *National water quality program*. U. S. Geological Survey Data Release. https://doi.org/10.5066/F7TX3CKP

Friedman, J. H. (2001). Greedy function approximation: A gradient boosting machine. *Annals of Statistics*, *29*(5), 1189–1232. https://doi.org/10.1214/aos/1013203451

Galloway, J. N., & Cowling, E. B. (2021). Reflections on 200 years of nitrogen, 20 years later. *Ambio*, *50*(4), 745–749. https://doi.org/10.1007/s13280-020-01464-z

Gao, Y., Tian, Y., Zhan, W., Li, L., Sun, H., Zhao, T., et al. (2023). Characterizing legacy nitrogen-induced time lags in riverine nitrogen reduction for the Songhuajiang River Basin: Source analysis, spatio-seasonal patterns, and impacts on future water quality improvement. *Water Research*, *242*(120292), 120292. https://doi.org/10.1016/j.watres.2023.120292

Gilbert, M., Nicolas, G., Cinardi, G., Van Boeckel, T. P., Vanwambeke, S. O., Wint, G. R. W., & Robinson, T. P. (2018). Global distribution data for cattle, buffaloes, horses, sheep, goats, pigs, chickens and ducks in 2010. *Scientific Data*, *5*(1), 180227. https://doi.org/10.1038/sdata.2018.227

Glibert, P. M. (2020). From hogs to HABs: Impacts of industrial farming in the US on nitrogen and phosphorus and greenhouse gas pollution. *Biogeochemistry*, *150*(2), 139–180. https://doi.org/10.1007/s10533-020-00691-6

Goyette, J.-O., Bennett, E. M., Howarth, R. W., & Maranger, R. (2016). Changes in anthropogenic nitrogen and phosphorus inputs to the st. Lawrence sub-basin over 110 years and impacts on riverine export. *Global Biogeochemical Cycles*, *30*(7), 1000–1014. https://doi.org/10.1002/2016GB005384

23284277, 2026, 8, Downloaded from https://agupubs.onlinelibrary.wiley.com/doi/10.1029/2026EF008532, Wiley Online Library on [03/11/2026]. See the Terms and Conditions (https://onlinelibrary.wiley.com/terms-and-conditions) on Wiley Online Library for rules of use; OA articles are governed by the applicable Creative Commons License

Han, H., & Allan, J. D. (2008). Estimation of nitrogen inputs to catchments: Comparison of methods and consequences for riverine export prediction. *Biogeochemistry*, *91*(2), 177–199. https://doi.org/10.1007/s10533-008-9279-3

Han, J., Destouni, G., Jarsjö, J., Zhang, Q., Cantoni, J., & Zhang, C. (2024). Legacy sources determine current water quality: Nitrogen and phosphorus in streams of Australia, China, Sweden and USA. *The Science of the Total Environment*, *954*(176407), 176407. https://doi.org/10.1016/j.scitotenv.2024.176407

Han, Y., Feng, G., Swaney, D. P., Dentener, F., Koeble, R., Ouyang, Y., & Gao, W. (2020). Global and regional estimation of net anthropogenic nitrogen inputs (NANI). *Geoderma*, *361*, 114066. https://doi.org/10.1016/j.geoderma.2019.114066

Hansen, A. T., Dolph, C. L., Foufoula-Georgiou, E., & Finlay, J. C. (2018). Contribution of wetlands to nitrate removal at the watershed scale. *Nature Geoscience*, *11*(2), 127–132. https://doi.org/10.1038/s41561-017-0056-6

Harding, L. W., Jr., Mallonee, M. E., Perry, E. S., Miller, W. D., Adolf, J. E., Gallegos, C. L., & Paerl, H. W. (2019). Long-term trends, current status, and transitions of water quality in Chesapeake Bay. *Scientific Reports*, *9*(1), 6709. https://doi.org/10.1038/s41598-019-43036-6

Hastie, T., Tibshirani, R., & Friedman, J. (2009). *The elements of statistical learning: Data mining, inference, and prediction, second edition*. Springer Science & Business Media.

Helsel, D. R., Hirsch, R. M., Ryberg, K. R., Archfield, S. A., & Gilroy, E. J. (2020). *Statistical methods in water resources (no. 4-A3)*. U.S. Geological Survey. https://doi.org/10.3133/tm4A3

Hirsch, R. M., & DeCicco, L. A. (2015). User guide to exploration and graphics for RivEr trends (EGRET) and dataRetrieval: R packages for hydrologic data. In *Techniques and methods*. US Geological Survey. https://doi.org/10.3133/tm4a10

Hirsch, R. M., DeCicco, L. A., & Murphy, J. (2021). *Exploration and graphics for RivEr trends (EGRET) (3.0.5)*. U.S. Geological Survey. Retrieved from https://pubs.usgs.gov/tm/04/a10/

Hong, B., Swaney, D. P., McCrackin, M., Svanbäck, A., Humborg, C., Gustafsson, B., et al. (2017). Advances in NANI and NAPI accounting for the Baltic drainage basin: Spatial and temporal trends and relationships to watershed TN and TP fluxes. *Biogeochemistry*, *133*(3), 245–261. https://doi.org/10.1007/s10533-017-0330-0

Howarth, R., Swaney, D., Billen, G., Garnier, J., Hong, B., Humborg, C., et al. (2012). Nitrogen fluxes from the landscape are controlled by net anthropogenic nitrogen inputs and by climate [Dataset]. *Frontiers in Ecology and the Environment*, *10*(1), 37–43. https://doi.org/10.1890/100178

Howarth, R. W., Billen, G., Swaney, D., Townsend, A., Jaworski, N., Lajtha, K., et al. (1996). Regional nitrogen budgets and riverine N & P fluxes for the drainages to the North Atlantic Ocean: Natural and human influences. In *Nitrogen cycling in the North Atlantic Ocean and its watersheds* (pp. 75–139). https://doi.org/10.1007/978-94-009-1776-7_3

Huishu, L., Qiuliang, L., Xinyu, Z., Haw, Y., Hongyuan, W., Limei, Z., et al. (2018). Effects of anthropogenic activities on long-term changes of nitrogen budget in a plain river network region: A case study in the Taihu Basin. *The Science of the Total Environment*, *645*, 1212–1220. https://doi.org/10.1016/j.scitotenv.2018.06.354

Johnson, H. M., & Stets, E. G. (2020). Nitrate in streams during winter low-flow conditions as an indicator of legacy nitrate. *Water Resources Research*, *56*(11), e2019WR026996. https://doi.org/10.1029/2019WR026996

Lark, T. J., Hendricks, N. P., Smith, A., Pates, N., Spawn-Lee, S. A., Bougie, M., et al. (2022). Environmental outcomes of the US renewable fuel standard. *Proceedings of the National Academy of Sciences of the United States of America*, *119*(9), e2101084119. https://doi.org/10.1073/pnas.2101084119

Lefcheck, J. S., Orth, R. J., Dennison, W. C., Wilcox, D. J., Murphy, R. R., Keisman, J., et al. (2018). Long-term nutrient reductions lead to the unprecedented recovery of a temperate coastal region. *Proceedings of the National Academy of Sciences of the United States of America*, *115*(14), 3658–3662. https://doi.org/10.1073/pnas.1715798115

Liu, J., Van Meter, K. J., McLeod, M. M., & Basu, N. B. (2021). Checkered landscapes: Hydrologic and biogeochemical nitrogen legacies along the river continuum. *Environmental Research Letters*, *16*(11), 115006. https://doi.org/10.1088/1748-9326/ac243c

Lloret, J., & Valiela, I. (2016). Unprecedented decrease in deposition of nitrogen oxides over North America: The relative effects of emission controls and prevailing air-mass trajectories. *Biogeochemistry*, *129*(1–2), 165–180. https://doi.org/10.1007/s10533-016-0225-5

Lundberg, S. M., Erion, G., Chen, H., DeGrave, A., Prutkin, J. M., Nair, B., et al. (2020). From local explanations to global understanding with explainable AI for trees. *Nature Machine Intelligence*, *2*(1), 56–67. https://doi.org/10.1038/s42256-019-0138-9

Lundberg, S. M., & Lee, S.-I. (2017). A unified approach to interpreting model predictions. *Advances in Neural Information Processing Systems*, 4765–4774.

Malone, T. C., & Newton, A. (2020). The globalization of cultural eutrophication in the coastal ocean: Causes and consequences. *Frontiers in Marine Science*, *7*, 670. https://doi.org/10.3389/fmars.2020.00670

McDowell, R. W., Simpson, Z. P., Ausseil, A. G., Etheridge, Z., & Law, R. (2021). The implications of lag times between nitrate leaching losses and riverine loads for water quality policy. *Scientific Reports*, *11*(1), 16450. https://doi.org/10.1038/s41598-021-95302-1

Millard, S. P. (2013). *EnvStats: An R package for environmental statistics*. Springer Science & Business Media.

Murphy, J. C. (2020). Changing suspended sediment in United States Rivers and streams: Linking sediment trends to changes in land use/cover, hydrology and climate. *Hydrology and Earth System Sciences*, *24*(2), 991–1010. https://doi.org/10.5194/hess-24-991-2020

Oelsner, G. P., Sprague, L. A., Murphy, J. C., Zuellig, R. E., Johnson, H. M., Ryberg, K. R., et al. (2017). Water-quality trends in the nation's rivers and streams, 1972–2012—Data preparation, statistical methods, and trend results. In *Scientific investigations report*. https://doi.org/10.3133/sir20175006

Oelsner, G. P., & Stets, E. G. (2019). Recent trends in nutrient and sediment loading to coastal areas of the conterminous U.S.: Insights and global context. *Science of The Total Environment*, *654*, 1225–1240. https://doi.org/10.1016/j.scitotenv.2018.10.437

Patakamuri, S. K., & O'Brien, N. (2021). Modifiedmk: Modified versions of Mann Kendall and Spearman's rho trend tests. https://cran.r-project.org/web/packages/modifiedmk/index.html

Pei, W., Yan, T., Lei, Q., Zhang, T., Fan, B., Du, X., et al. (2022). Spatio-temporal variation of net anthropogenic nitrogen inputs (NANI) from 1991 to 2019 and its impacts analysis from parameters in Northwest China. *Journal of Environmental Management*, *321*, 115996. https://doi.org/10.1016/j.jenvman.2022.115996

Perry, M. T. (2023). Rasterstats python package (0.18.0). https://github.com/perrygeo/python-rasterstats

Rabalais, N. N., Turner, R. E., & Scavia, D. (2002). Beyond science into policy: Gulf of Mexico hypoxia and the Mississippi River: Nutrient policy development for the Mississippi River watershed reflects the accumulated scientific evidence that the increase in nitrogen loading is the primary factor in the worsening of hypoxia in the northern Gulf of Mexico. *BioScience*, *52*(2), 129–142. https://doi.org/10.1641/0006-3568(2002)052[0129:BSIPGO]2.0.CO;2

Ransom, K. M., Nolan, B. T., Stackelberg, P. E., Belitz, K., & Fram, M. S. (2021). Machine learning predictions of nitrate in groundwater used for drinking supply in the conterminous United States. *The Science of the Total Environment*, *807*, 151065. https://doi.org/10.1016/j.scitotenv.2021.151065

23284277, 2026, 8, Downloaded from https://agupubs.onlinelibrary.wiley.com/doi/10.1029/2026EF008532, Wiley Online Library on [03/11/2026]. See the Terms and Conditions (https://onlinelibrary.wiley.com/terms-and-conditions) on Wiley Online Library for rules of use; OA articles are governed by the applicable Creative Commons License

Rowland, F. E., Stow, C. A., Johnson, L. T., & Hirsch, R. M. (2021). Lake Erie tributary nutrient trend evaluation: Normalizing concentrations and loads to reduce flow variability. *Ecological Indicators*, *125*, 107601. https://doi.org/10.1016/j.ecolind.2021.107601

Sabo, R. D., Clark, C. M., Bash, J., Sobota, D., Cooter, E., Dobrowolski, J. P., et al. (2019). Decadal shift in nitrogen inputs and fluxes across the contiguous United States: 2002–2012. *Journal of Geophysical Research: Biogeosciences*, *124*(10), 3104–3124. https://doi.org/10.1029/2019jg005110

Sabo, R. D., Sullivan, B., Wu, C., Trentacoste, E., Zhang, Q., Shenk, G. W., et al. (2022). Major point and nonpoint sources of nutrient pollution to surface water have declined throughout the Chesapeake Bay watershed. *Environmental Research Communications*, *4*(4), 1–11. https://doi.org/10.1088/2515-7620/ac5db6

Sadayappan, K., Kerins, D., Shen, C., & Li, L. (2022). Nitrate concentrations predominantly driven by human, climate, and soil properties in US Rivers. *Water Research*, *226*, 119295. https://doi.org/10.1016/j.watres.2022.119295

Schilling, K. E., Streeter, M. T., Vogelgesang, J., Jones, C. S., & Seeman, A. (2020). Subsurface nutrient export from a cropped field to an agricultural stream: Implications for targeting edge-of-field practices. *Agricultural Water Management*, *241*, 106339. https://doi.org/10.1016/j.agwat.2020.106339

Sobota, D. J., Harrison, J. A., & Dahlgren, R. A. (2009). Influences of climate, hydrology, and land use on input and export of nitrogen in California watersheds. *Biogeochemistry*, *94*(1), 43–62. https://doi.org/10.1007/s10533-009-9307-y

Sprague, L. A., Mitchell, R. M., Pollard, A. I., & Falcone, J. A. (2019). Assessing water-quality changes in US Rivers at multiple geographic scales using results from probabilistic and targeted monitoring. *Environmental Monitoring and Assessment*, *191*(6), 348. https://doi.org/10.1007/s10661-019-7481-5

Stackpoole, S. M., Sabo, R., Falcone, J., & Sprague, L. A. (2021). Long-term Mississippi River trends expose shifts in the River load response to watershed nutrient balances between 1975 and 2017. *Water Resources Research*, *57*(11), e2021WR030318. https://doi.org/10.1029/2021WR030318

Stackpoole, S. M., Stets, E. G., & Sprague, L. A. (2019). Variable impacts of contemporary versus legacy agricultural phosphorus on US River water quality. *Proceedings of the National Academy of Sciences of the United States of America*, *116*(41), 20562–20567. https://doi.org/10.1073/pnas.1903226116

Stets, E. G., Sprague, L. A., Oelsner, G. P., Johnson, H. M., Murphy, J. C., Ryberg, K., et al. (2020). Landscape drivers of dynamic change in water quality of U.S. Rivers. *Environmental Science & Technology*, *54*(7), 4336–4343. https://doi.org/10.1021/acs.est.9b05344

Swaney, D. P., Hong, B., Ti, C., Howarth, R. W., & Humborg, C. (2012). Net anthropogenic nitrogen inputs to watersheds and riverine N export to coastal waters: A brief overview. *Current Opinion in Environmental Sustainability*, *4*(2), 203–211. https://doi.org/10.1016/j.cosust.2012.03.004

Swaney, D. P., Howarth, R. W., & Hong, B. (2018). Nitrogen use efficiency and crop production: Patterns of regional variation in the United States, 1987–2012. *The Science of the Total Environment*, *635*, 498–511. https://doi.org/10.1016/j.scitotenv.2018.04.027

Tesoriero, A. J., Wherry, S. A., Dupuy, D. I., & Johnson, T. D. (2024). Predicting redox conditions in groundwater at a national scale using random forest classification. *Environmental Science & Technology*, *58*(11), 5079–5092. https://doi.org/10.1021/acs.est.3c07576

U.S. Environmental Protection Agency (USEPA). (2020). National Rivers and streams assessment 2013–2014: A collaborative survey. *US EPA*. Retrieved from www.epa.gov/national-aquatic-resource-surveys/national-rivers-and-streams-assessment-2013-2014-report

Valayamkunnath, P., Barlage, M., Chen, F., Gochis, D. J., & Franz, K. J. (2020). Mapping of 30-meter resolution tile-drained croplands using a geospatial modeling approach. *Scientific Data*, *7*(1), 257. https://doi.org/10.1038/s41597-020-00596-x

Van Meter, K. J., & Basu, N. B. (2015). Catchment legacies and time lags: A parsimonious watershed model to predict the effects of legacy storage on nitrogen export. *PLoS One*, *10*(5), e0125971. https://doi.org/10.1371/journal.pone.0125971

Van Meter, K. J., & Basu, N. B. (2017). Time lags in watershed-scale nutrient transport: An exploration of dominant controls. *Environmental Research Letters*, *12*(8), 084017. https://doi.org/10.1088/1748-9326/aa7bf4

Van Meter, K. J., Basu, N. B., & Van Cappellen, P. (2017). Two centuries of nitrogen dynamics: Legacy sources and sinks in the Mississippi and Susquehanna River Basins. *Global Biogeochemical Cycles*, *31*(1), 2–23. https://doi.org/10.1002/2016GB005498

Van Meter, K. J., Byrnes, D. K., & Basu, N. B. (2023). Memory and management: Competing controls on long-term nitrate trajectories in U.S. Rivers. *Global Biogeochemical Cycles*, *37*(4), e2022GB007651. https://doi.org/10.1029/2022gb007651

Van Meter, K. J., Van Cappellen, P., & Basu, N. B. (2018). Legacy nitrogen may prevent achievement of water quality goals in the Gulf of Mexico. *Science*, *360*(6387), 427–430. https://doi.org/10.1126/science.aar4462

Vero, S. E., Basu, N. B., Van Meter, K. J., Richards, K. G., Mellander, P.-E., Healy, M. G., & Fenton, O. (2017). Review: The environmental status and implications of the nitrate time lag in Europe and North America. *Hydrogeology Journal*, *26*, 1–16. https://doi.org/10.1007/s10040-017-1650-9

Wang, A., Tang, L., Yang, D., & Lei, H. (2016). Spatio-temporal variation of net anthropogenic nitrogen inputs in the upper Yangtze River basin from 1990 to 2012. *Science China Earth Sciences*, *59*(11), 2189–2201. https://doi.org/10.1007/s11430-016-0014-6

Ward, M. H., Jones, R. R., Brender, J. D., de Kok, T. M., Weyer, P. J., Nolan, B. T., et al. (2018). Drinking water nitrate and human health: An updated review. *International Journal of Environmental Research and Public Health*, *15*(7), 1557. https://doi.org/10.3390/ijerph15071557

Williams, T. J., Klager, B. J., & Stiles, T. C. (2024). Water-quality trends in the Kansas River, Kansas, since enactment of the clean water act, 1972–2020. In *Scientific investigations report (no. 2024–5050)*. US Geological Survey. https://doi.org/10.3133/sir20245050

Wolock, D. M. (2003). Base-flow index grid for the conterminous United States. https://databasin.org/datasets/d8c2b299681c486e8d6daf98aac10cfe

XGBoost Python Package—xgboost 0.90 documentation. (n.d.). XGBoost python package—Xgboost 0.90 documentation. Retrieved from https://federated-xgboost.readthedocs.io/en/latest/python/index.html

Yuan, P., Li, H., Yi, X., Wang, J., Ning, C., Xu, X., & Nong, X. (2025). Optimizing water quality index using machine learning: A six-year comparative study in riverine and reservoir systems. *Scientific Reports*, *15*(1), 33919. https://doi.org/10.1038/s41598-025-10187-8

Yue, S., & Wang, C. Y. (2004). The Mann-Kendall test modified by effective sample size to detect trend in serially correlated hydrological series. *Water Resources Management*, *18*(3), 201–218. https://doi.org/10.1023/B:WARM.0000043140.61082.60

Zhang, Q., Bostic, J. T., & Sabo, R. D. (2022). Regional patterns and drivers of total nitrogen trends in the Chesapeake Bay watershed: Insights from machine learning approaches and management implications. *Water Research*, *218*(118443), 118443. https://doi.org/10.1016/j.watres.2022.118443

Zhang, Q., Hirsch, R. M., DeCicco, L. A., & Murphy, J. C. (2026). Fifteen years of WRTDS for advancing water-quality science: A review of methodological developments and global applications. *Environmental Science & Technology*, *60*(15), 11170–11182. https://doi.org/10.1021/acs.est.5c12895

Zhang, X., Zou, T., Lassaletta, L., Mueller, N. D., Tubiello, F. N., Lisk, M. D., et al. (2021). Quantification of global and national nitrogen budgets for crop production. *Nature Food*, *2*(7), 529–540. https://doi.org/10.1038/s43016-021-00318-5

23284277, 2026, 8, Downloaded from https://agupubs.onlinelibrary.wiley.com/doi/10.1029/2026EF008532, Wiley Online Library on [03/11/2026]. See the Terms and Conditions (https://onlinelibrary.wiley.com/terms-and-conditions) on Wiley Online Library for rules of use; OA articles are governed by the applicable Creative Commons License

Zhao, Q., Peng, B., Ma, Z., Jia, M., McIsaac, G. F., Robertson, D. M., et al. (2025). How do hydrological variability and human activities control the spatiotemporal changes of riverine nitrogen export in the upper Mississippi River basin? *Environmental Science & Technology*, *60*(1), 1028–1039. https://doi.org/10.1021/acs.est.5c06476

Zhong, W., Wang, S., Dong, Y., Ni, Z., Fan, Y., & Wu, D. (2022). Trends of the response-relationship between net anthropogenic nitrogen and phosphorus inputs (NANI/NAPI) and TN/TP export fluxes in Raohe basin, China. *Chemosphere*, *286*(1), 131662. https://doi.org/10.1016/j.chemosphere.2021.131662

Zomer, R., & Trabucco, A. (2022). Global aridity index and potential evapotranspiration (ET0) database: Version 6 [Dataset]. *figshare*. https://doi.org/10.6084/M9.FIGSHARE.7504448.V6

23284277, 2026, 8, Downloaded from https://agupubs.onlinelibrary.wiley.com/doi/10.1029/2026EF008532, Wiley Online Library on [03/11/2026]. See the Terms and Conditions (https://onlinelibrary.wiley.com/terms-and-conditions) on Wiley Online Library for rules of use; OA articles are governed by the applicable Creative Commons License